IJITCE

ISSN 2347- 3657

International Journal of Information Technology & Computer Engineering

Email : ijitce.editor@gmail.com or editor@ijitce.com

International Journal of Information Technology & Computer Engineering

ISSN 2347–3657

Volume 6, Issue 3, 2018

Theoretical Modeling of an Artificial Magnetic Conductor with Three Bands

Suma G C, Vidhya B, Madhvaraja K

Asst. Prof, Asst. Prof, Asst. Prof

sumasavita@gmail.com, vidhyab.rymec@gmail.com, madhavaraja@pdit.ac.in

Department of EEE, Proudhadevaraya Institute of Technology, Abheraj Baldota Rd, Indiranagar, Hosapete, Karnataka-583225

Abstract

Because of their intricate architecture, analytical modelling of artificial magnetic conductors is necessary for understanding and optimising their behaviour. A three-band AMC that reflects incident waves at 1.21 GHz, 1.61 GHz, and 2.46 GHz in phase is shown in this work. The layout is a tripartite square loop, with one square loop controlling each frequency. Furthermore, a mathema tical model is suggested for the purpose of forecasting the AMC's operational frequencies.

Keywords: Artificial Magnetic Conductor, Frequency Selective Surface, Transmission Line Model

1. Introduction

Artificial magnetic conductor is a type of metamaterial that exhibits properties similar to a perfect magnetic conductor [1]. Due to its ability to reflect incident waves with zero reflection phase, it has been implemented in many antenna designs as a back reflector to enhance their gain. The complexity of AMC structures makes it challenging to model them through analytical methods, and in most previous publications, full-wave simulation was the main analytical approach. Nevertheless, analytical methods remain of great interest and need to be explored.

In this paper, a triple-band AMC based on a square loop structure is introduced, where each frequency can be controlled independently, facilitating its design. Moreover, an analytical model is proposed that predicts where the three null reflection phases occur. Section 2 will present the triple-band AMC designalong with its analytical model. In Section 3, a comparison between simulation and modeled results will be shown and discussed. Finally, a conclusion will be drawn in Section 4.

2. The Triple-Band AMC

• Design

The triple-band AMC unit cell (shown in Figure 1) is based on [2], where the structure is composed of three square loops with dimensions d_1 = 22.29mm, w_1 = 0.305mm, d_2= 21.68mm, w_2= 2.14mm, d_3 = 15.64mm, w_3 = 4.32mm, printed on a substrate with relative permittivity ε_r = 10.2 and dimensions p = 25mm, h = 5mm. The AMC operates at three frequencies, where each frequency is controlled by one square loop respectively.

To obtain the reflection phase diagram of the AMC shown in Figure 2a, a unit cell model in CST Microwave Studio software using the frequency domain solver with periodic boundary

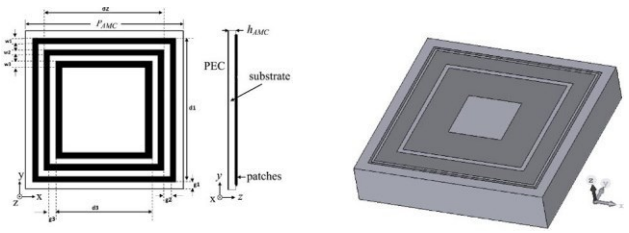

(a) Geometry (b) Unit cell

Figure 1: The Proposed Triple-Band AMC

Conditions was simulated. A perfect magnetic and electric conducting wall was imposed on ±y and ±x directions, respectively. The waveguide port was placed in the far-field region and was used to excite the signal along +z while perfect electric (E_t = 0) was applied due to a full ground along –z.

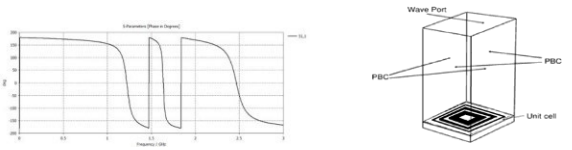

(a) Reflection phase diagram. (b) Simulation setup.

Figure 2: Simulation Overview: Setup and Results

These boundary conditions were used to imitate the periodic nature of the structure (Figure 2b). The simulation results show resonance at 1.21 GHz, 1.61 GHz, and 2.46 GHz, at which the AMC can reflect incident waves with a zero-reflection phase, having the same characteristics as PMC.

International Journal of Information Technology & Computer Engineering

ISSN 2347–3657

Volume 6, Issue 3, 2018

2.1 Analytical Model

To model the proposed triple-band AMC analytically, a transmission line model is established Figure 3. The AMC is divided into a frequency selective surface (FSS) and a slab treated as a spacing medium between the FSS and the ground plane [3]. The surface impedance Z_s is then calculated from the parallel connection of the FSS grid impedance Z_g and the slab impedance Z_d:

$$Z_s = \frac{Z_g Z_d}{Z_g + Z_d} \tag{1}$$

The reflection coefficient is then computed as:

$$\Gamma^{TE} = \frac{Z_s \cos\theta - \eta_0}{Z_s \cos\theta + \eta_0}, \quad \Gamma^{TM} = \frac{Z_s - \eta_0 \cos\theta}{Z_s + \eta_0 \cos\theta} \tag{2}$$

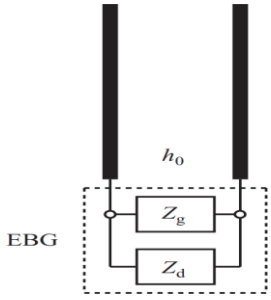

Figure 3: Equivalent Transmission Line Model for Plane Wave Incidences [3].

Where η_0 is the free space wave impedance and θ is the incidentangle. The resonant frequency for the zero-degree reflection phase must satisfy:

$$X_g(\omega_0) + X_d(\omega_0) = 0 \tag{3}$$

$$X_g(\omega_0) = \mathrm{Im}(Z_g),\ X_d(\omega_0) = \mathrm{Im}(Z_d)$$

Z_d is simply the input impedance of a TEM line section of length$h$, and in most interesting cases $kdh \ll 1$, both $Z_{d\mathrm{TE}}$ and $Z_{d\mathrm{TM}}$ are practically equal [4,5].

$$Z_d^{\mathrm{TE,\ TM}} \approx j\omega\mu_0 h \tag{4}$$

The grid impedance Z_g of the FSS depends on the specific geometry used in the design. In our case, the triple-square loop ismodeled using the equivalent circuit approach (shown in Figure 4). For transverse electrical (TE) wave incidence, the vertical strips act as an L impedance, and the horizontal gratings as a C impedance [6,7].

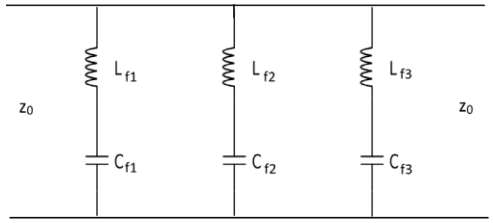

Figure 4: Equivalent Circuit Model of the Triple Square Loop FSS

The basic equations for calculating the values of inductance and capacitance are found in Marcuvitz [8] and are given in general form by:

$$\text{Inductance: } \frac{X_L}{Y_0} = \omega L = \frac{d}{p}\cos\vartheta F(p, s, \lambda) \tag{5}$$

$$\text{Capacitance: } \frac{Z_0 B}{Y_0} = \omega C = \frac{4d}{p}\sec\vartheta F(p, s, \lambda)\varepsilon_{\mathrm{eff}} \tag{6}$$

$$\text{where: } F(p, s, \lambda) = \frac{p}{\lambda}\ln\csc\frac{\pi s}{2p} + G(p, s, \lambda) \tag{7}$$

And G is the correction term:

$$G(p, s, \lambda) = \frac{\left(1 - \frac{\beta^2}{4}\right)^2 \left(1 - \frac{\beta^2}{2}\right)(A_+ + A_-) + 4\beta^2 A_+ A_-}{\frac{1}{2}\left(1 - \frac{\beta^2}{4}\right) + \beta^2\left(1 + \frac{\beta^2}{2} - \frac{\beta^4}{8}\right)(A_+ + A_-) + 2\beta^6 A_+ A_-} \tag{8}$$

The six circuit elements given in Figure 4: L_{f1}, C_{f1}, L_{f2}, C_{f2}, L_{f3}, C_{f3}, are calculated as follows:

$$L_{f1} = \frac{2 \cdot (L_1 \parallel L_2) \cdot d_1}{p}, \quad C_{f1} = \frac{0.75 \cdot C_1 \cdot d_1 \cdot \varepsilon_{\mathrm{eff}}}{p} \tag{10}$$

$$L_{f2} = \frac{L_3 \cdot d_2}{p}, \quad C_{f2} = \frac{(C_1 \text{ in series with } C_2) \cdot d_2 \cdot \varepsilon_{\mathrm{eff}}}{p} \tag{11}$$

$$L_{f3} = \frac{1.455 \cdot L_4 \cdot d_3}{p}$$

$$C_{f3} = \frac{(C_1 \text{ in series with } C_2 \text{ in series with } C_3) \cdot d_3 \cdot \varepsilon_{\mathrm{eff}}}{p} \tag{12}$$

Where:

$$\begin{aligned} L_1 &= F(p, w_1, \lambda),\ C_1 = 4F(p, 2g_1, \lambda), \\ L_2 &= F(p, w_2, \lambda),\ C_2 = 4F(p, g_2, \lambda), \\ L_3 &= F(p, 2w_2, \lambda),\ C_3 = 4F(p, g_3, \lambda), \\ L_4 &= F(p, 2w_3, \lambda) \end{aligned} \tag{13}$$

The factor $\varepsilon_{\mathrm{eff}}$ present in Equation (6) was introduced by Munk [9] with the value of $\varepsilon_{\mathrm{eff}} = 0.5(\varepsilon_r + 1)$.

It is important to note that the equations presented here have certain conditions that need to be respected to obtain correct results, such as $s/p \ll 1$, $p/\lambda \ll 1$, and $p(1 + \sin\theta)/\lambda < 1$.

3. Results and Discussion

By solving Equation (3) for the proposed dimensions, we obtain the three frequencies predicted by the analytical model: 1.21 GHz, 1.61 GHz, 2.46 GHz, which are identical to the electromagnetic (EM) simulation.

To further investigate the analytical model and demonstrate how different parameters affect the resonance frequencies, a parametric study is conducted and shown in Figure 5.

The parametric study reveals that the three resonant frequencies, f_1, f_2, f_3, of the artificial magnetic conductor (AMC) are highly dependent on the square sides d_1, d_2, d_3 respectively, and on the substrate characteristics such as thickness h and permittivity ε_r. The results also demonstrate that varying one frequency does not significantly affect the other two frequencies, and sometimes

they remain unchanged. This independence allows tuning one frequency by altering the dimensions of the corresponding square loop without affecting the remaining frequencies, greatly facilitating the design process.

Lastly, the analytical model successfully predicted the three resonant frequencies for most cases. The root-mean-square error (RMSE) has been calculated for the complete parametric

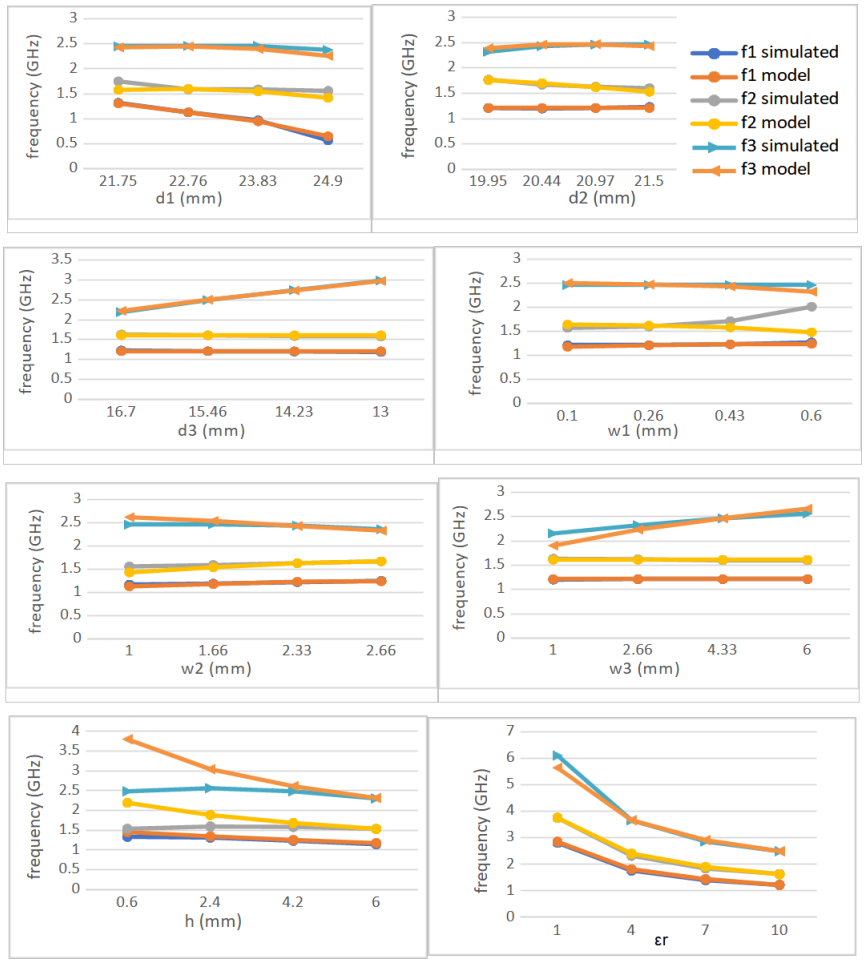

Figure 5: Results of the Parametric Study on the Triple-Band AMC

Study, where the frequencies predicted by the model were evaluated against the electromagnetic (EM) simulation, and the results are shown in Figure 6.

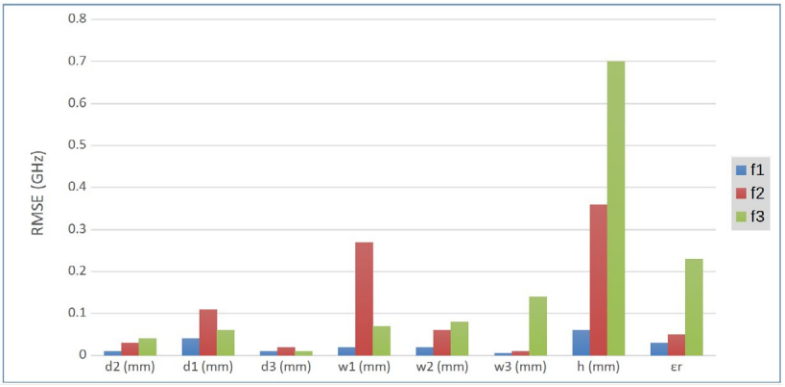

Figure 6: RMSE Evaluation for Each Parameter

ISSN 2347–3657

Volume 6, Issue 3, 2018

The figure shows that the analytical model has the least accuracy when it comes to the thickness parameter. Moreover, the third frequency has the highest error among all three frequencies, so more work needs to be done to improve the model.

4. Conclusion

A new unit cell for Artificial Magnetic Conductors (AMCs) with three bands is suggested in this article. An important design benefit is that it may be independently adjusted to reflect incident waves in phase at one of three operational frequencies: 1.21 GHz, 1.61 GHz, or 2.46 GHz. The tri-band AMC is also modelled analytically. This model outperforms the complete wave simulation in predicting the AMC operating frequencies, with an error estimate below 170 MHz.

References

1. Sievenpiper, D., Zhang, L., Broas, R. F., Alexopolous, N. G., & Yablonovitch, E. (1999). High-impedance electromagnetic surfaces with a forbidden frequency band. *IEEE Transactions on Microwave Theory and techniques, 47*(11), 2059-2074.
2. Fattouche, A., Mouffok, L., Hebib, S., & Mansoul, A. (2022). A triple band artificial magnetic conductor: design & analytical model. *Progress In Electromagnetics Research Letters, 104,* 161-168.
3. Yang, F., & Rahmat-Samii, Y. (2008). Electromagnetic band gap structures in antenna engineering (pp. 156-201). Cambridge, UK: Cambridge university press.
4. Tretyakov, S. (2003). Analytical modeling in applied electromagnetics. Artech House.
5. Simovski, C. R., de Maagt, P., & Melchakova, I. V. (2005). High-impedance surfaces having stable resonance with respect to polarization and incidence angle. *IEEE transactions on antennas and propagation, 53*(3), 908-914.
6. Langley, R. J., & Parker, E. A. (1982). Equivalent circuit model for arrays of square loops. *Electronics Letters, 18*, 294-296.
7. Langley, R. J., & Parker, E. A. (1983). Double-square frequency-selective surfaces and their equivalent circuit. *Electronics Letters, 17*(19), 675-677.
8. Marcuvitz, N. (1951). Waveguide handbook (No. 21). Iet.
9. Munk, B. A. (2005). Frequency selective surfaces: theory and design. John Wiley & Sons.